Effect of Pore Pressure on the Velocity of Compressional Waves in Low-Porosity Rocks

TERRY TODD AND GENE SIMMONS

Department of Earth and Planetary Sciences, Massachusetts Institute of Technology Cambridge, Massachusetts 02139

The velocity V_p of compressional waves has been measured in rock samples of low porosity to confining pressures P_c of 2 kb for a number of different constant pore pressures P_p. An effective pressure defined by $P_e = P_c - nP_p$, $n \leq 1$, is found to be the determining factor in the behavior of V_p rather than an effective pressure defined simply by the differential pressure $\Delta P = P_c - P_p$. As pore pressure increases at constant effective pressure, the value of n increases and approaches 1, but as effective pressure increases at constant pore pressure, the value of n decreases. These observations are consistent with Biot's theory of the propagation of elastic waves in a fluid-saturated porous solid.

In the past decade several physical properties of low-porosity crystalline rocks have been measured under confining pressures to 10 kb. Large changes in these physical properties over the first 1–2 kb (Figure 1) have been attributed to the closing of long thin microcracks in the rocks. A further indication of the presence of these microcracks was found by *Nur and Simmons* [1969*a*], who reported that at these low confining pressures the compressional velocity of fully saturated samples is greater than the velocity of dry samples by 20–30%. Other authors have studied changes that take place in the compressional velocity of high-porosity sandstones when pore pressure is introduced into saturated samples already under confining pressure. On the basis of experimental data for sandstones of 15–30% porosity, *Hicks and Berry* [1956], *Wyllie et al.* [1958], and *King* [1966] suggest that the compressional velocity is determined simply by the differential pressure $\Delta P = P_c - P_p$; *Gardner et al.* [1965] give a brief theoretical discussion supporting this view. On the other hand, theoretical works by *Brandt* [1955] and *Biot* [1956*a*, *b*] suggest that an effective pressure $P_e = P_c - nP_p$, where $n \leq 1$, is the determining factor in the behavior of compressional velocity. *Brandt* [1955], *Fatt* [1959], and *Banthia et al.* [1965] support this view on the basis of their experimental work with high-porosity sandstones. With these contradictory viewpoints in mind, we investigate the role that pore pressure plays in determining compressional velocity in low-porosity crystalline rocks.

SYMBOLS AND DEFINITIONS

The following symbols and definitions will be used:

- P_p pore pressure, bars.
- P_c confining pressure, bars.
- P_e effective pressure, bars, equal to $P_c - nP_p$, where $n \leq 1$.
- ΔP differential pressure, bars, equal to $P_c - P_p$.
- V_p compressional velocity, kilometers per second.
- V_s shear velocity, kilometers per second.
- β compressibility, per bar.
- τ_{ij} stress component on a unit cube of jacketed material, bars; summation convention applies.
- ϵ_{ij} strain component on a unit cube of jacketed material.
- e $= \sum_i e_{ii}$.
- $\mathbf{u}$ displacement of matrix material, centimeters.
- $\mathbf{U}$ displacement of fluid, centimeters.
- ϵ $= \sum_i \partial U_i/\partial x_i$.
- ϕ porosity.
- μ, λ isothermal Lamé constants, bars.
- Ψ $= -$ div $\mathbf{U}$.
- M $[\phi\beta_f + \beta_r(1 - \phi) - (\beta_r^2/\beta_B)]^{-1}$, bars.
- n $= 1 - (\beta_r/\beta_B)$.
- β_f, β_r, β_B fluid, unjacketed, and jacketed compressibilities, respectively, per bar.

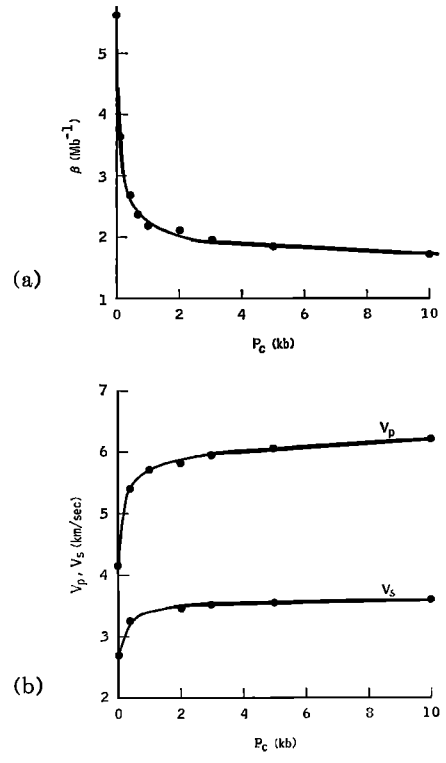

Fig. 1. (*a*) Compressibility of Westerly granite as a function of confining pressure [*Simmons and Brace*, 1965]. (*b*) Compressional and shear velocity as a function of confining pressure [*Simmons and Brace*, 1965].

ρ = $\rho_s(1 - \phi) + \rho_f\phi$, grams per cubic centimeter.
ρ_s, ρ_f solid and fluid densities, respectively, grams per cubic centimeter.
m mass coupling factor.
η fluid viscosity, poise.
$F(f)$ complex function of frequency.
k permeability, nanodarcy.
f_t frequency above which Poiseuille flow breaks down, per second.
κ dimensionless mass coupling factor.
z dimensionless root of determinantal equation 26.
V_{sd} shear velocity of dry sample, kilometers per second.
V_{ss} shear velocity of wet sample, kilometers per second.
V_{p1}, V_{p2} compressional velocities predicted by Biot's theory, kilometers per second.

EQUIPMENT

The basic measurement is that of traveltime of an elastic pulse through a rock sample. The pulse is produced by applying an electrical signal across a piezoelectric transducer located at one end of the sample; the output signal is picked up by another transducer located at one opposite end of the sample. The electronic equipment is similar to that described by *Birch* [1960] and *Simmons* [1964].

The pressure system (Figure 2) can attain

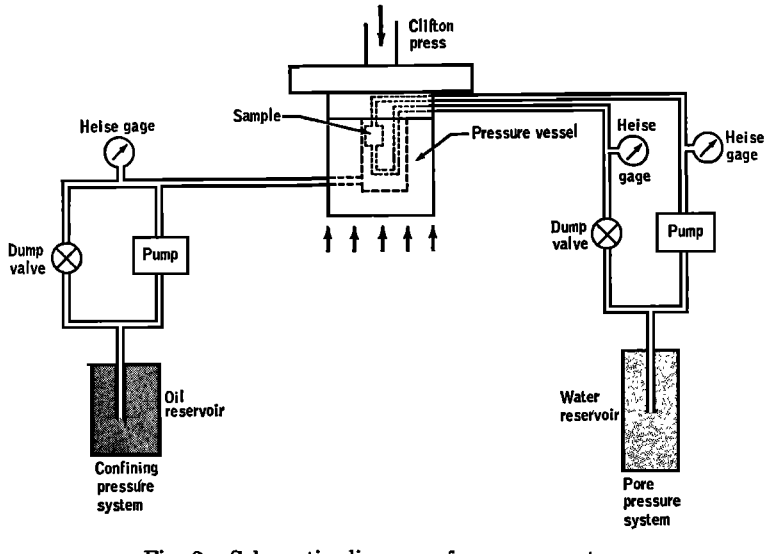

Fig. 2. Schematic diagram of pressure system.

confining pressures of 2 kb. The confining pressure medium is hydraulic oil, and the pressure is measured with Heise bourdon gages. Extending through the lid of the pressure vessel are six electrical leads and two pressure fittings through which the pore fluid is transmitted. A separate hydraulic system is used to apply pore pressure to the sample, independent of confining pressure. The pore pressure medium is water, and again Heise bourdon gages are used.

Each sample is a cylinder 4 inches in diameter and about 1 inch thick; the ends are ground parallel to ±0.001 inch. The transducer assembly (Figure 3) consists of two stainless steel backing pieces 4 inches in diameter and 1 inch thick. A hole 1 inch in diameter has been cut 0.75 inch into the center of one side of each disc; the bottom of this hole is parallel to the opposite face. A 1-MHz barium titanate transducer is placed on the bottom of this hole, a copper disc connected to the input electrical cable is set on the transducer, and a glass plug is clamped down on the transducer to hold it tight against the stainless steel. The grounded electrical cable is attached to the backing piece. When the input pulse is applied to the copper disc, the backing piece acts as a second electrode and generates the acoustic signal in the transducer. The time delay of the elastic signal through the specimen carriage, the electronic equipment, the electrical leads, and so forth is automatically subtracted by clamping the backing pieces face to face under pressure and zeroing the delay line. Because the compressional velocity of stainless steel varies by a negligible amount over the pressure range of 2 kb, this procedure provides a constant zero from which the delay time in the sample can be determined. The pore pressure fluid is introduced through the backing piece into a series of interpenetrating crosshatched grooves so that water is in contact with about a third of the surface of the rock. To prevent any unnecessary distortion of the signal, no grooves were cut directly across from the transducer. A section of gum rubber tubing is slipped over the whole carriage and clamped to the backing pieces. This flexible jacket allows us to apply a hydrostatic confining pressure to the sample, independent of the pore pressure inside the sample.

ERROR ANALYSIS

The accuracy of our results depends primarily on four measurements: confining pressure, pore pressure, sample length, and delay time in sample. The accuracy of the Heise gages is ±0.5%. The sample length is known to ±0.001 inch (±0.1%). Corrections have not

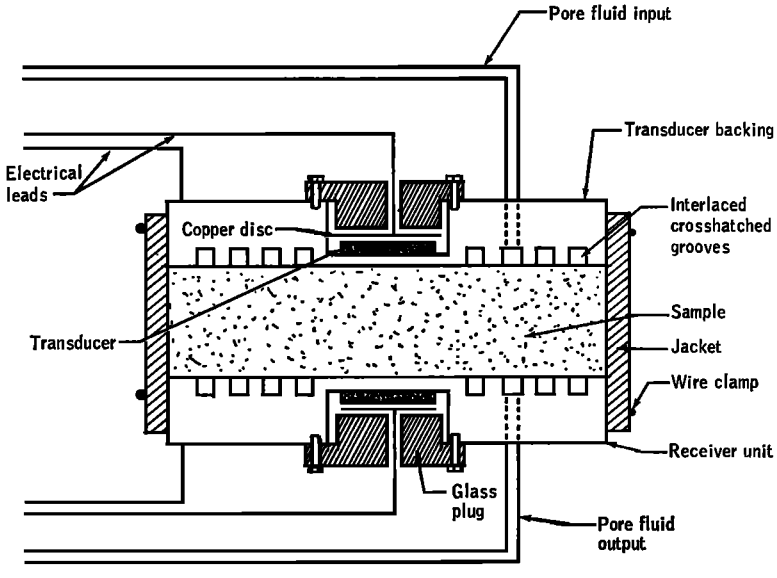

Fig. 3. Schematic diagram of sample assembly.

been applied for changes in sample length with pressure due to compressibility; these corrections would amount to about 0.3% at 2 kb. An accurate measurement of the delay time in the sample depends on the ability of the experimenter to pick the first arrival in the wave train and to relate this arrival to the time at which the input pulse was applied. The chief limitation is the gradual arrival of the first signal [*Birch*, 1960], which can be determined only to about 2% relative to the initial input pulse. However, a consistent choice of the onset of this first arrival yields a precision of about 0.2% in one value relative to the next.

Aside from these sources of possible error that arise in taking the measurements, we have sources associated with the assumption of pressure equilibrium in the rock. That is, to what precision can we characterize the system by one (P_c, P_p, V_p) value? The three basic problems here are incomplete saturation, low permeability, and hysteresis.

There are two steps involved in our saturation process. In the first step the sample is placed in a vacuum oven at 10^{-2} torr and 80°C for at least 24 hours. Then, without reducing the vacuum, water is introduced into the vacuum chamber, and the sample, which is still immersed in water, is jacketed (Figure 3). In the second step water is pumped under pressure through the rock. The confining and the input pore pressures are raised to 100 bars, and the output pore pressure is monitored until it too reads 100 bars. Over the span of a few hours the pore and the confining pressures are lowered together to atmospheric pressure before the first reading is taken. We found that this process gave us the maximum value for compressional velocity at atmospheric pressure. Recycling in a similar manner with pore pressures to 1050 bars or applying these high pore pressures to the sample for a period of 1–2 days gave no further increase in the value of V_p. We interpret these maximum V_p values as being due to the greatest degree of saturation that we could attain in the laboratory at the pressures we have used.

Figure 4 illustrates the results of a simple experiment showing the effect of the low permeability of Trigg limestone on velocity measurements after a rapid change in confining pressure. The confining pressure of a sample

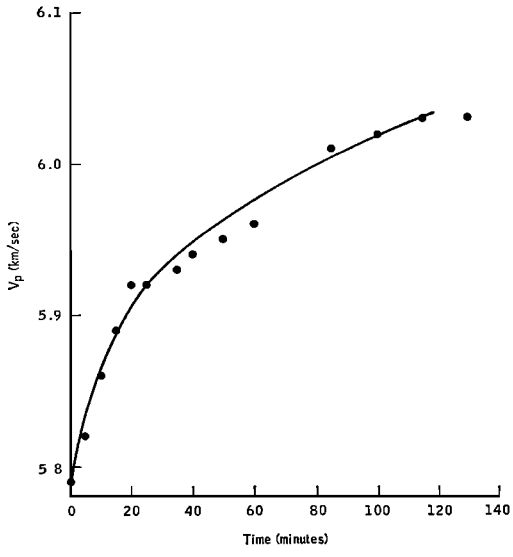

Fig. 4. A demonstration of the low permeability of Trigg limestone 9077L. The increase in compressional velocity is shown as a function of time when confining pressure has been reduced at $t = 0$ from $P_c = 2000$ bars ($P_p = 0$ bars, $V_p = 6.4$ km/sec) to $P_c = 100$ bars ($P_p = 0$ bars). The compressional velocity for a dry sample at $P_c = 100$ bars is 5.2 km/sec. For a saturated sample in equilibrium at $P_c = 100$ bars and $P_p = 0$ bars, the compressional velocity is 6.1 km/sec.

in equilibrium at $P_c = 2000$ bars ($P_p = 0$ bars, $V_p = 6.4$ km/sec) was quickly reduced to 100 bars, and the velocity monitored as a function of time. The value of V_p sharply decreased as the confining pressure rapidly decreased. Then, over the span of a few hours, V_p slowly increased and approached the expected velocity value (6.1 km/sec) of the saturated sample in equilibrium at a confining pressure of 100 bars. We interpret the sharp drop in the value of V_p as being due to cracks reopening throughout the rock but not refilling immediately with water. Because of the low permeability of the rock, several hours are needed for water to reach some of these cracks. The rate of increase in the value of V_p is a measure of the rate at which the cracks are being refilled. Moreover, when a nonzero pore pressure is introduced into the sample, a similar problem of attaining equilibrium in pore pressure throughout the sample arises. The input and output gages on the pore pressure system were designed to provide a check on this pore pressure

equilibrium; pumping water into one side of the rock under pressure and monitoring the pressure buildup on the other side provided the test that we needed to tell when the pore pressure had attained equilibrium in those cracks reached by the pore fluid. At high effective pressures we often had to wait more than 2 days for the input and output gages to reach equilibrium. Whether the pore fluid reached all the cracks and, if not, whether it would if more time were allowed are questions we have not answered.

A final point of interest is the hysteresis involved in a typical pressure run [*Gardner et al.*, 1965]. The form that hysteresis usually takes in velocity measurements is that the decreasing pressure values of V_p fall above the increasing pressure values. *Gardner et al.* [1965] have shown that, when hysteresis cycles are present, the compressional velocity depends not only on the values of pore and confining pressures but also on the past pressure history. Gardner et al. also show for high-porosity sandstones that, if hysteresis effects are eliminated, the value of compressional velocity is determined simply by the differential pressure $\Delta P = P_c - P_p$. If hysteresis effects are introduced into the velocity data systematically [*Banthia et al.*, 1965], the value of V_p becomes dependent on an effective pressure $P_e = P_c - nP_p$, $n \leq 1$.

With these arguments in mind we investigate hysteresis effects in our measurements. The first readings for the Chelmsford granite were taken for increasing confining pressure at zero pore pressure. After attaining 2 kb, the confining pressure was reduced, again for zero pore pressure. The whole cycle took more than a week to complete. We did see a hysteresis loop, but the maximum deviation of the decreasing pressure values from the increasing pressure values was <1% (*Gardner et al.* [1965, Figure 1] show a hysteresis loop of about 5% for the Berea sandstone). Similar cycles for pore pressure >0 showed even less hysteresis. These small hysteresis loops can be attributed to (1) waiting a number of hours between readings (*Gardner et al.* [1965] have suggested that at least part of the reason for their large hysteresis loops is a short wait of only 10 min between readings), and (2) pumping water through the rock under pressure (because an increase in confining pressure also brought on an increase in pore pressure, the output pore pressure had to be lowered to allow some water to flow through the rock and return the over-all pore pressure to the initial value). The hysteresis effects can be reduced further by choosing only increasing confining pressure values, as we have done in Tables 1–3.

NUMERICAL DATA

The Chelmsford granite sample was cored from a larger sample brought back to the laboratory. This granite was described previously by *Dale* [1908, 1923], *Chayes* [1952], and *Birch* [1960]. The Trigg limestone samples are cores obtained during the drilling of a well by the Mobil Oil Company at a location 8 km northwest of Irving, Texas. The number after the Trigg sample is the depth in feet from which the core came. The values of the properties of these specimens are listed below.

Chelmsford Granite

1. Density (dry): 2.619 g/cm³.
2. Porosity: 0.005.
3. Modal analysis (per cent volume): quartz, 31%; potash feldspar (microcline), 31%; plagioclase (oligoclase), 31%; mica (biotite), 1%; mica (muscovite), 4%; chlorite, 2%.

TABLE 1. Velocity of Compressional Waves in Chelmsford Granite

P_c, bars	Velocity, km/sec					
	P_p=0	P_p=100	P_p=300	P_p=500	P_p=750	P_p=1050
0	5.254					
50	5.498					
100	5.563	5.450				
150		5.563				
200	5.689	5.659				
300	5.758	5.732	5.463			
350			5.614			
400			5.640			
500	5.893	5.909	5.780			
550				5.540		
600				5.601		
700				5.711		
750	5.967	5.976	5.934		5.521	
800					5.592	
850				5.783		
900					5.750	
1000	6.043	6.026	6.009		5.849	
1050				5.946		5.606
1100						5.671
1200						5.837
1300	6.105	6.113	6.095		5.942	
1400				6.052		
1500						5.961
1600	6.148	6.147	6.139	6.114	6.049	
2000	6.202	6.184	6.184	6.184	6.139	6.125

P_c, confining pressure. P_p, pore pressure in bars.

TABLE 2. Velocity of Compressional Waves in Trigg Limestone 9762B

P_c, bars	Velocity, km/sec					
	P_p=0	P_p=100	P_p=300	P_p=500	P_p=750	P_p=1050
0	5.432					
50	5.512					
100	5.596	5.388				
150		5.550				
200	5.688	5.598				
300	5.777	5.769	5.420			
350			5.579			
400		5.836	5.643			
500	5.983	5.891	5.810	5.495		
550				5.677		
600			5.927	5.742		
700				5.823		
750	6.079	6.044	5.947		5.488	
800				5.914	5.635	
850					5.697	
900					5.861	
1000	6.132	6.205	6.151	6.098	5.924	
1050						5.516
1100						5.700
1300	6.235	6.219	6.158	6.106	6.015	5.847
1400						5.922
1600	6.296	6.299	6.279	6.224	6.148	6.027
2000	6.370	6.352	6.326	6.314	6.261	6.224

P_c, confining pressure. P_p, pore pressure in bars.

4. Remarks: modal analysis from *Birch* [1960] on a different sample.

Trigg Limestone 9762B

1. Density (dry): 2.767 g/cm³.
2. Porosity: 0.005.
3. Modal analysis (per cent volume): carbonate, 95%; quartz, 5%; ore trace.
4. Remarks: carbonate grains ≪0.1 mm in size. Some of the carbonate has recrystallized to single crystals ¼ to 5 mm in size and occupying about 5% of the thin section. Quartz occurs as rounded and very occasionally subangular grains, usually <¼ mm in size and inhomogeneously distributed throughout the thin section.

The velocity data are presented in Tables 1–3. Confining pressure, pore pressure, and compressional velocity are included. The value of V_p is given to four significant figures. The accuracy of these values is only about 2%; the precision of one reading relative to another is about 0.2%. In this sense the inclusion of the last significant figure has merit.

Discussion of Experimental Results

Our data for the Chelmsford granite are illustrated in Figures 5–7. The first diagram shows compressional velocity as a function of confining pressure for a number of different constant pore pressures. The other diagrams compare the velocity data for the pressures

$$\Delta P = P_c - P_p \tag{1}$$

$$P_e = P_c - nP_p \qquad n \leq 1 \tag{2}$$

The first effective pressure is the differential pressure. If the compressional velocity is determined by the differential pressure only, each contour in Figure 6 should align with the zero pore pressure contour. However, the data scatter 3–4% and show a systematic shift of all nonzero pore pressure contours to the low-pressure side of the zero pore pressure contour. Because the precision of our data, including hysteresis effects, is about ±1%, we believe the 3–4% systematic deviation is significant. We therefore choose an n value for each pore pressure contour such that, when compressional velocity is plotted as a function of effective pressure $P_e = P_c - nP_p$, the best fit to the zero pore pressure contour is obtained (Figure 7). By introducing this effective pressure, the systematic overcorrection has been eliminated, and the scatter in V_p values has been reduced to about 1%; this scatter is more in line with the precision expected from our measure-

TABLE 3. Velocity of Compressional Waves in Trigg Limestone 9762B

P_c, bars	Velocity, km/sec				
	P_p=80	P_p=280	P_p=480	P_p=730	P_p=1030
100	5.478				
150	5.562				
200	5.618				
300	5.768	5.500			
350		5.598			
400	5.838	5.656			
500	5.896	5.818	5.614		
550			5.688		
600		5.931	5.743		
700			5.820		
750	6.076	5.973		5.561	
800			5.926	5.629	
850				5.711	
900				5.849	
1000	6.181	6.151	6.101	5.931	
1050					5.612
1100					5.732
1300	6.228	6.192	6.107	6.030	5.871
1400					5.921
1600	6.298	6.279	6.231	6.137	6.038
2000	6.355	6.332	6.312	6.261	6.211

P_c, confining pressure. P_p, pore pressure in bars.

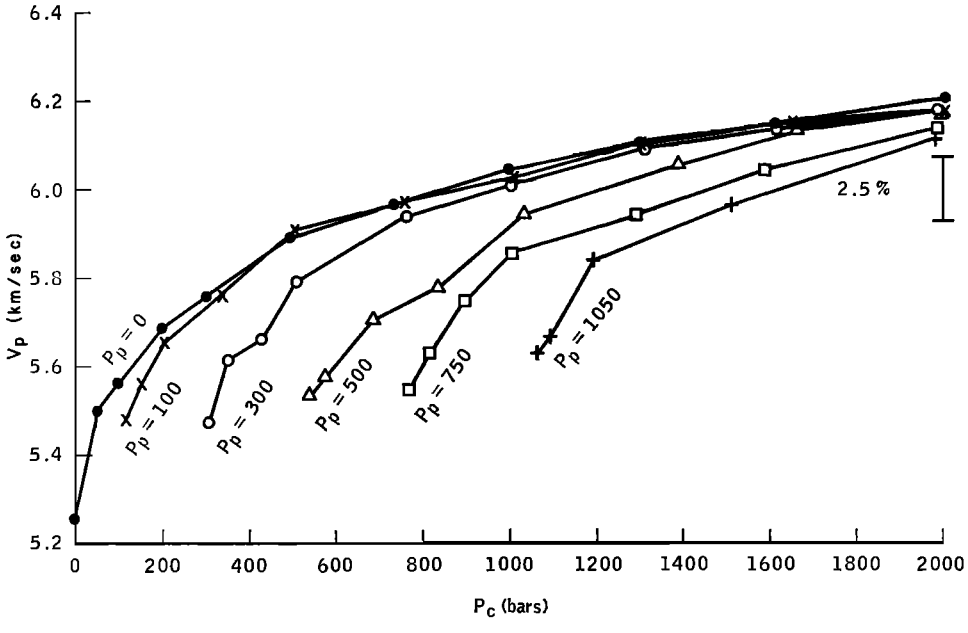

Fig. 5. Compressional velocity as a function of confining pressure for Chelmsford granite. A number of constant pore pressure contours are given.

ments. The n values so chosen were found to increase with pore pressure. Furthermore, the nonzero pressure contours in Figure 7 lie to the high-pressure side of the zero pore pressure contour at low effective pressures, whereas the same contours tend to lie to the low-pressure side of the zero pore pressure contour at high effective pressure. This relation implies that at constant pore pressure the value of n is smaller for higher differential pressures. Our data for

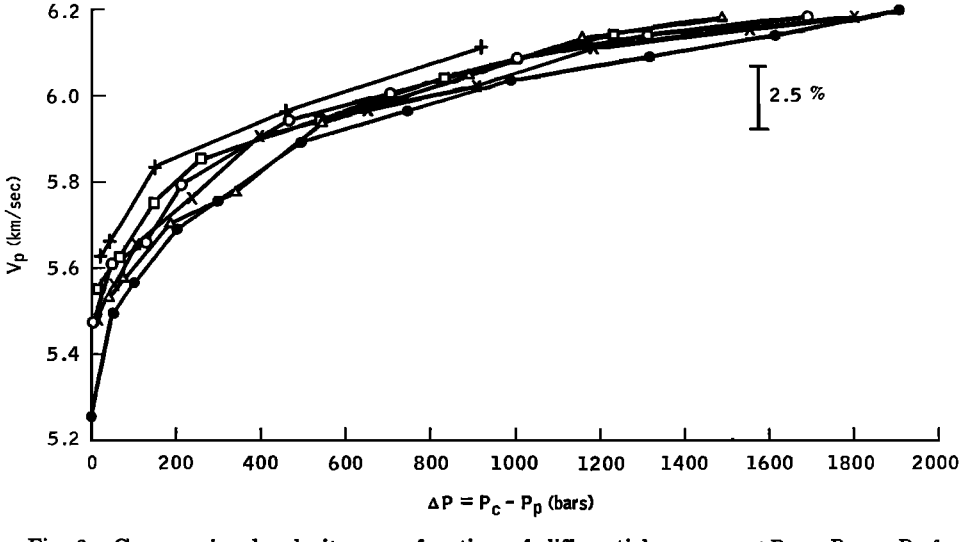

Fig. 6. Compressional velocity as a function of differential pressure $\Delta P = P_c - P_p$ for Chelmsford granite. Solid circles indicate $P_p = 0$ bars; crosses, $P_p = 100$ bars; open circles, $P_p = 300$ bars; triangles, $P_p = 500$ bars; squares, $P_p = 750$ bars; pluses, $P_p = 1050$ bars.

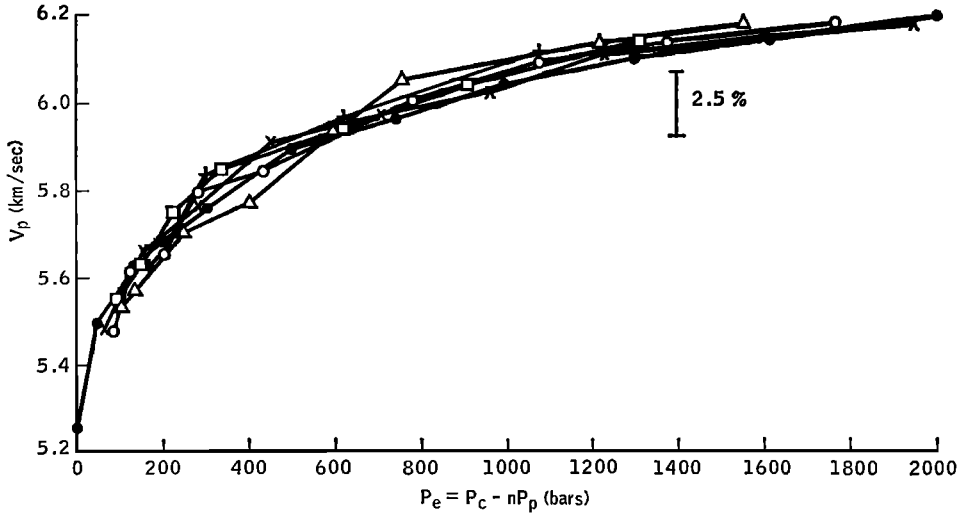

Fig. 7. Compressional velocity as a function of effective pressure $P_e = P_c - nP_p$, $n \leq 1$, for Chelmsford granite. Solid circles indicate $P_p = 0$; crosses, $P_p = 100$ bars and $n = 0.50$; open circles, $P_p = 300$ bars and $n = 0.75$; triangles, $P_p = 500$ bars and $n = 0.88$; squares, $P_p = 750$ bars and $n = 0.90$; pluses, $P_p = 1050$ bars and $n = 0.85$.

two runs on the Trigg limestone (Tables 2 and 3) show the same behavior displayed by the Chelmsford granite.

What can be said about this parameter n? We have plotted the value of n as a function of pore pressure for the two rocks we have studied (Figure 8); an error bar of about 10% can be attached to each data point. Even with this uncertainty the value of n is definitely not 1 throughout; thus we reject the simple differential pressure dependence for V_p expressed by (1). We are then forced to introduce an effective pressure characterized by this pressure-dependent parameter n. We will attempt to illustrate in a simplified way how a value of n different from 1 can arise.

For a small change in pressure an incremental change in the compressional velocity can be expressed as

$$dV_p = \left(\frac{\partial V_p}{\partial P_p}\right)_{\Delta P} dP_p + \left(\frac{\partial V_p}{\partial(\Delta P)}\right)_{P_p} d(\Delta P) \quad (3)$$

Assume for the moment that each individual grain in the rock is a perfect elastic crystal and that the pore pressure exerts a uniform compression on each grain. Then $(\partial V_p/\partial P_p)_{\Delta P}$ is a measure of the change in the compressional velocity of the individual grains with hydrostatic pore pressure at constant $P_c - P_p$, and $[\partial V_p/\partial(\Delta P)]_{P_p}$ is the change in the compressional velocity of the whole rock with a change in $P_c - P_p$ at constant pore pressure. Experimental observations suggest that at low values of $P_c - P_p$ we can make the approximation

$$\left(\frac{\partial V_p}{\partial P_p}\right)_{\Delta P} \ll \left(\frac{\partial V_p}{\partial(\Delta P)}\right)_{P_p} \quad (4)$$

The velocity dependence becomes

$$dV_p = \left(\frac{\partial V_p}{\partial(\Delta P)}\right)_{P_p} d(\Delta P) \quad (5)$$

and the differential pressure ΔP becomes the determining factor in the behavior of compressional velocity. *Gardner et al.* [1965] use similar arguments to predict this differential pressure dependence for velocity, and they present experimental data for sandstones under confining pressures to 135 bars to support their theory. On the other hand, at extremely high differential pressures ($P_c \gg P_p$), the two pressure derivatives are equal:

$$\left(\frac{\partial V_p}{\partial(\Delta P)}\right)_{P_p} = \left(\frac{\partial V_p}{\partial P_p}\right)_{\Delta P} \quad (6)$$

The velocity dependence becomes

$$dV_p = \left(\frac{\partial V_p}{\partial P_c}\right)_{P_p} dP_c \quad (7)$$

and, as is expected, the compressional velocity behaves like the velocity of a nonporous solid. However, here we are interested in intermediate differential pressures where the value of $(\partial V_p/\partial P_p)_{\Delta P}$ is a few per cent of the value of $[\partial V_p/\partial(\Delta P)]_{P_p}$. Here, when (3) is rearranged, the velocity dependence becomes

$$dV_p = \left(\frac{\partial V_p}{\partial(\Delta P)}\right)_{P_p} \cdot \left\{dP_c - \left[1 - \frac{(\partial V_p/\partial P_p)_{\Delta P}}{(\partial V_p/\partial(\Delta P))_{P_p}}\right] dP_p\right\} \quad (8)$$

and the compressional velocity is determined by an effective pressure

$$P_e = P_c - nP_p$$

$$n = 1 - \frac{(\partial V_p/\partial P_p)_{\Delta P}}{[\partial V_p/\partial(\Delta P)]_{P_p}} \quad (9)$$

Thus this simplified model predicts a pressure-dependent n value. This prediction is in accord with the more complete theory developed by Biot.

APPLICATION OF BIOT'S THEORY

In a series of papers [*Biot*, 1941, 1955, 1956*a*, *b*, *c*, 1962*a*, *b*; *Biot and Willis*, 1957], Biot developed a theory of deformation and a theory of acoustic wave propagation for a porous elastic solid containing a compressible fluid. To provide a framework in which to discuss the implications of Biot's theory for the interpretation of our data, we outline briefly the development of the theory and state explicitly the assumptions inherent in it.

The relations between stress and strain in porous material, including fluid pressure and dilatation, are first established. These relations are

$$\tau_{ij} - nP_p = 2\mu e_{ij} + \lambda e \qquad i \neq j \quad (10)$$

$$\tau_{ij} = \mu e_{ij} \qquad i \neq j \quad (11)$$

$$\Psi = \phi(e - \epsilon) = -(P_p/M) + ne \quad (12)$$

where τ_{ij} is the stress component on a unit cube of jacketed material and the summation convention applies.

$$e_{ij} = \frac{\partial u_i}{\partial x_j} + \frac{\partial u_j}{\partial x_i} \qquad i \neq j \quad (13)$$

$$e_{ii} = \partial u_i/\partial x_i \quad (14)$$

$$e = \sum_i e_{ii} \quad (15)$$

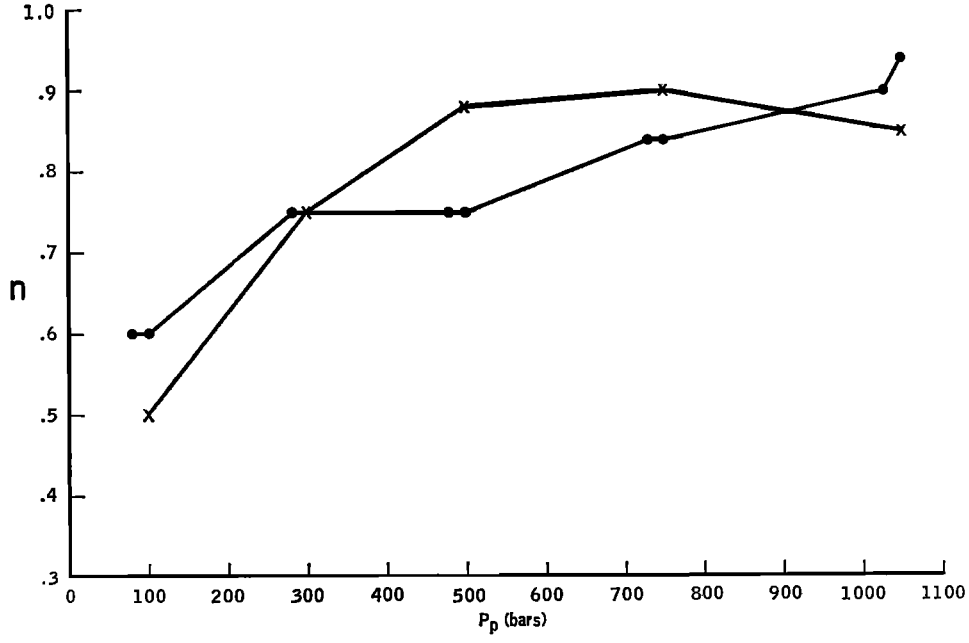

Fig. 8. The parameter n from the effective pressure $P_e = P_c - nP_p$ as a function of pore pressure for Chelmsford granite (crosses) and Trigg limestone 9762B (circles).

where $\mathbf{u}$ is the displacement of the matrix material.

$$\epsilon = \sum_i \partial u_i/\partial x_i \qquad (16)$$

Here $\mathbf{U}$ is the displacement of the fluid, ϕ is the porosity, μ and λ are the isothermal Lamé constants for the matrix material, P_p is the hydrostatic pore pressure, and $\Psi = -\operatorname{div}\mathbf{U}$. Physically Ψ is a measure of the amount of fluid that has flowed into or out of a given element of bulk material.

$$M = [\phi\beta_f + \beta_r(1-\phi) - (\beta_r^2/\beta_B)]^{-1} \qquad (17)$$

$$n = 1 - (\beta_r/\beta_B) \qquad (18)$$

where β_f, β_r, and β_B are the fluid, unjacketed, and jacketed compressibilities, respectively.

In the next step Biot wrote the dynamic relations and included specifically fluid viscosity, dissipation due to fluid friction, apparent or dynamic mass, and dynamic coupling between fluid and solid. The equations of motion are

$$\mu\nabla^2\mathbf{u} + (\lambda + n^2M + \mu)\nabla(e) - nM\nabla(\Psi) = \frac{\partial^2}{\partial t^2}(\rho\mathbf{u} + \rho_f\mathbf{U}) \qquad (19)$$

$$\nabla(nMe - M\Psi) = \frac{\partial^2}{\partial t^2}(\rho_f\mathbf{u} + m\mathbf{U}) + \frac{\eta F(f)}{k}\frac{\mathbf{U}}{t} \qquad (20)$$

where

$$\rho = \rho_s(1-\phi) + \rho_f\phi \qquad (21)$$

where ρ_s and ρ_f are the solid (matrix) and liquid densities, respectively, m is the mass coupling factor, η is the fluid viscosity, $F(f)$ is a complex function of frequency, and k is the permeability of the porous material.

In solving these equations for rotational and compressional waves, Biot considered two frequency ranges: $f < f_t$ and $f > f_t$, where f_t is a critical frequency at which Poiseuille flow breaks down. (Poiseuille flow implies that the inertial forces of the viscous fluid are negligible in comparison with the forces applied to the fluid.) One rotational and two compressional waves were found to exist, a result contrary to that expected for wave propagation in a homogeneous isotropic elastic medium where only one compressional wave exists. A simple physical explanation is based on a consideration of the relative motions of solid and liquid. For one compressional wave V_{p1} the motions of the solid and the liquid are in phase; for the other wave V_{p2} the motions are out of phase. Because of the low velocity and the high attenuation of the V_{p2} waves, the V_{p1} compressional wave and the rotational wave carry most of the acoustic energy. The shear velocity V_s is

$$V_s = (\mu/\rho)^{1/2} \qquad f \ll f_t \qquad (22)$$

$$V_s = \{\mu/[\rho - (\rho_f\phi/\kappa)]\}^{1/2} \qquad f \gg f_t \qquad (23)$$

where κ is a dimensionless mass coupling factor ($\kappa = 3$ for a random arrangement of pores). For low porosity rocks ($\phi \leq 1\%$) the difference between the two velocities is negligible. The compressional velocity V_{p1} is

$$V_{p1} = [(\lambda + 2\mu + n^2M)/\rho]^{1/2} \qquad f \ll f_t \qquad (24)$$

$$V_{p1} = \{[(\lambda + 2\mu + n^2M)/\rho]z\}^{1/2} \qquad f \gg f_t \qquad (25)$$

where z is a frequency-dependent term given by the largest root of the equation

$$\begin{vmatrix} z-1 & \dfrac{nM}{\lambda+2\mu+n^2M} - \dfrac{\rho_f}{\rho}z \\ \dfrac{nM}{\lambda+2\mu+n^2M} - \dfrac{\rho_f}{\rho}z & \dfrac{\rho_f}{\rho}\dfrac{\kappa}{\phi}z - \dfrac{M}{\lambda+2\mu+n^2M} \end{vmatrix} = 0$$

King [1966] showed that for realistic values of liquid and bulk compressibilities, pore-pore interactions, dynamic coupling of pore fluid and solid, and pore shape the value of z is always within 1–2% of 1 in high-porosity rocks (ϕ = 10–20%). For low-porosity rocks ($\phi < 1\%$) the value of z differs from 1 by $<1\%$. Hence dispersion is small in low-porosity rocks for both shear and compressional waves.

But what are the assumptions involved in the derivation of these equations?

1. The wavelength of the elastic waves must be greater than the characteristic size of the largest grain or pore. On a scale length comparable to the wavelength of the elastic waves the rock must be isotropic and elastic; any cut through the sample must contain the same proportion of liquid and solid. In our measure-

ments we have used a frequency of 1 MHz, which corresponds to a wavelength of about ½ cm. Most grains and hence crack lengths along grain boundaries in our samples have a maximum dimension of 0.1 cm. Therefore this assumption of scale size in relation to wavelength of elastic waves is satisfied in our experimental work.

2. The pores must be completely filled with liquid; i.e., saturation must be complete. We described in detail the experimental technique that we used to secure complete saturation. We believe but have not proved by an independent test that saturation was essentially complete.

3. Elastic hysteresis must be absent. This phenomenon, discussed in the text, was small in effect. It was $\leq 1\%$ in every case. We believe that this value is small enough to satisfy the assumption.

4. The pore fluid must be viscous and compressible; in addition, it must be of a density comparable to that of the solid matrix and must be able to flow relative to the solid. Our pore fluid is water. At low frequencies water has all these properties. Although it might appear that the response of water to high-frequency signals is a possible invalidation of this set of assumptions, Biot has considered this limit in his special case of a fluid without viscosity and found that the response of fluids to high-frequency signals has little effect on changing velocities.

5. A final assumption is the frequency dependence of seismic velocities. The effect of frequency on velocity is negligible for $f < f_t$, and for realistic values of the various parameters involved [*Biot*, 1956*a*, *b*] the compressional velocity can vary with frequency by a few per cent at most for $f > f_t$. A width of a few microns implies $f_t = 10^6$ Hz [*King*, 1966]. Our working frequency of 1 MHz is thus close to $f = f_t$.

These assumptions of Biot's theory appear to be met by our samples and our experimental arrangement. What then are the implications of this theory? Equation 10 implies that, for a hydrostatic pressure $P_c = \tau_{ii}$, where $\tau_{ij} = 0$ if $i \neq j$, a pore pressure $P_p = P_c/n$ is required to eliminate strains introduced in the solid matrix by P_c. In other words, the deformation of the solid matrix is determined by a pressure $P_c - nP_p$. What then does static deformation say about compressional velocity? At pressures below 2 kb, compressional velocity is determined to a large extent by the closing of cracks. The closing of cracks is determined by (10). In this sense V_p is determined by an effective pressure $P_c - nP_p$, $n = 1 - (\beta_r/\beta_s)$.

A significant part of the pressure dependence of V_p might be due to the effect of changes in the fluid compressibility β_f. The parameter β_f is contained in the n^2M and z terms of (25). Estimated values for the change in the value of n^2M due to the change in β_f with pressure suggest that for Westerly granite at $P_c = P_p = 0$ the value of V_p is about 4% lower than it would be for 'incompressible' water. An increase in $P_c - P_p$ or P_p reduces the discrepancy between the two velocities. At $P_c = P_p = 2$ kb, V_p is about 2% lower than it would be for incompressible water. At $P_c - P_p = 2$ kb the effect of fluid compressibility on velocity is negligible. The effect of β_f on V_p through z is similar but smaller [*King*, 1966]. The net result is that the value of V_p plotted as a function of differential pressure $P_c - P_p$ increases with pore pressure. This effect is in the same direction as that predicted from the $P_c - nP_p$ relation discussed earlier.

It appears that we have two pressure effects: the effect due to the closing of cracks, which suggests a pressure dependence defined by $P_c - nP_p$, and the effect due to changes in fluid compressibility with pressure, which involves a pressure dependence through the more complicated n^2M and z terms. The sizes of the two effects are of the same order of magnitude, and the pressure dependence of velocity for the two effects is in the same direction.

With these arguments in mind, what can be said about the applicability of Biot's theory to acoustic wave propagation in low-porosity crystalline rocks where the pore space is in the form of cracks? *King* [1966] has examined the applicability of Biot's theory to sedimentary rocks. A number of his measurements suggest that Biot's theory applies to sedimentary rocks, but he finds one discrepancy. Biot's theory predicts that the shear velocity of dry samples V_{sd} is always greater than that of saturated samples V_{ss}. King finds that for about half of his samples $V_{sd} < V_{ss}$ at low P_c, whereas $V_{sd} > V_{ss}$ at high P_c. He assume that the anomalous

behavior at low P_e is caused by the relaxation behavior of the liquid in small cracks in the rocks. At high P_e these small cracks are closed, and only large 'spherical' pores are left open. He suggests that Biot's theory holds for the large spherical pores but not for the thin cracks. On the other hand, *Nur and Simmons* [1969*a*] have measured the shear velocities of dry and saturated samples of low porosity at zero pore pressure and confining pressures to 4 kb. Their results show typically that $V_{sd} < V_{ss}$ for $P_e <$ 200 bars and that $V_{sd} > V_{ss}$ for $P_e > 200$ bars, in agreement with King's observations. However, a large part of the pore space in most of Nur and Simmons' samples is in the form of long thin cracks. The fact that Biot's prediction that $V_{sd} > V_{ss}$ holds for these samples above 200 bars where long thin cracks are still present does not support King's suggestion for the cause of the low-pressure deviations. In view of the larger uncertainties in the measurement of velocity at low pressure we believe that the more precise high-pressure measurements indicate that Biot's theory does apply to velocity measurements in low-porosity rocks.

Our data show experimentally that V_p depends on the effective pressure $P_e = P_c - nP_p$ rather than on the differential pressure $\Delta P = P_c - P_p$. Biot demonstrated mathematically the same dependence. Our rocks and experimental conditions satisfy the requirements of his theory. Thus Biot reached the same conclusions from mathematical considerations that we have drawn from our experimental data.

CONCLUSION

For pore pressures <2 kb the effective pressure defined by $P_e = P_c - nP_p$, $n \leq 1$, is the determining factor in the behavior of compressional velocity rather than the differential pressure $\Delta P = P_c - P_p$. For constant effective pressure the value of n increases and approaches 1 at high pore pressure; for constant pore pressure the value of n decreases at high effective pressure. This behavior is consistent with the predictions of Biot's theory. Assuming the simple differential pressure dependence $n = 1$ results in overestimates of 3–4% in compressional velocity measurements.

Acknowledgments. We thank H. Wang, D. Weidner, and W. F. Brace for many helpful suggestions throughout the course of this work, S. Baldridge for analyzing the Trigg limestone, and D. Riach for helping design the pressure system. Core from the Trigg well was provided by the Mobil Oil Co., Field Research Laboratory, Duncanville, Texas.

The research was supported in part by NASA contract NAS 9-8102 and in part directly by the NASA Manned Spacecraft Center, Houston, Texas.

REFERENCES

Banthia, B. S., M. S. King, and I. Fatt, Ultrasonic shear wave velocities in rocks subjected to simulated overburden pressure and internal pore pressure, *Geophysics, 30,* 117, 1965.

Biot, M. A., General theory of three-dimensional consolidation, *J. Appl. Phys., 12,* 155, 1941.

Biot, M. A., Theory of elasticity and consolidation of a porous anisotropic solid, *J. Appl. Phys., 26,* 182, 1955.

Biot, M. A., Theory of propagation of elastic waves in a fluid-saturated solid, 1, Low frequency range, *J. Acoust. Soc. Amer., 28,* 162, 1956*a*.

Biot, M. A., Theory of propagation of elastic waves in a fluid-saturated solid, 2, Higher frequency range, *J. Acoust. Soc. Amer., 28,* 179, 1956*b*.

Biot, M. A., General solution of the equations of elasticity and consolidation for a porous material, *J. Appl. Mech., 23,* 91, 1956*c*.

Biot, M. A., Mechanics of deformation and acoustic propagation in porous media, *J. Appl. Phys., 33,* 1482, 1962*a*.

Biot, M. A., Generalized theory of acoustic propagation in porous media, *J. Acoust. Soc. Amer., 34,* 1254, 1962*b*.

Biot, M. A., and D. G. Willis, The elastic coefficients of the theory of consolidation, *J. Appl. Mech., 24,* 594, 1957.

Birch, F., The velocity of compressional waves in rocks to 10 kilobars, 1, *J. Geophys. Res., 65,* 1083, 1960.

Brandt, H., A study of the speed of sound in porous granular materials, *J. Appl. Mech., 22,* 479, 1955.

Chayes, F., The finer-grained calcalkaline granites of New England, *J. Geol., 60,* 207, 1952.

Dale, T. N., The chief commercial granites of Massachusetts, New Hampshire, and Rhode Island, *U.S. Geol. Surv. Bull., 354,* 1, 1908.

Dale, T. N., The commercial granites of New England, *U.S. Geol. Surv. Bull., 738,* 1, 1923.

Fatt, I., The Biot-Willis elastic coefficients for sandstone, *J. Appl. Mech., 26,* 296, 1959.

Gardner, G. H. F., M. R. J. Wyllie, and D. M. Droschak, Hysteresis in the velocity-pressure characteristics of rocks, *Geophysics, 30,* 111, 1965.

Hicks, W. G., and J. E. Berry, Application of continuous velocity logs to determination of fluid saturation of reservoir rocks, *Geophysics, 21,* 739, 1956.

King, M. S., Wave velocities in rocks as a func-

tion of changes in overburden pressure and pore fluid saturants, *Geophysics, 31,* 50, 1966.
Nur, A., and G. Simmons, The effect of saturation on velocity in low porosity rock, *Earth Planet. Sci. Lett., 7,* 183, 1969*a*.
Nur, A., and G. Simmons, The effect of viscosity of a fluid phase on velocity in low porosity rocks, *Earth Planet. Sci. Lett., 7,* 99, 1969*b*.
Simmons, G., Velocity of shear waves in rocks to 10 kilobars, 1, *J. Geophys. Res., 69,* 1123, 1964.
Simmons, G., and W. F. Brace, Comparison of static and dynamic measurements of compressibility of rocks, *J. Geophys. Res., 70,* 5649, 1965.
Wyllie, M. R. J., A. R. Gregory, and G. H. F. Gardner, An experimental investigation of factors affecting elastic wave velocities in porous media, *Geophysics, 23,* 459, 1958.

(Received July 21, 1971;
revised March 30, 1972.)